

Characterization of Chromium (VI) Interaction with Rivers Sediments-In Relation to the Composition

Sarah Azzouz^{1*}, Chahrazed Boukhalfa¹

¹ Laboratory of Pollution and Water Treatment, Chemistry Department, University Brothers Mentouri Constantine, Algeria

* Corresponding author's e-mail: azzouz_sarah@yahoo.fr

ABSTRACT

The aim of the present work is to evaluate the mobility of chromium (VI) in aquatic systems by studying its interaction with different rivers sediments. The studied sediments were collected from the river Essouk which flows through a mining area in Skikda, and from the river Hemimime which flows through an industrial area in Constantine. The Cr(VI) fixation experiments on the studied sediments were carried out in batch. The results obtained show that the fixation of Cr(VI) is mainly related to the composition of the sediments. Sediments with a predominance of schwertmannite fix Cr(VI) better. The predominance of jarosite or calcite in sediments, implies a low Cr(VI) retention capacity. In the three cases, the kinetics of Cr(VI) fixation follows the pseudo-second order kinetic model. The adsorption isotherm is best described by the Freundlich model in the case of the jarosite predominance and by the Langmuir model in the case of the schwertmannite or the calcite predominance.

Keywords: chromium (VI), sediments, adsorption, mobility, Essouk river, Hemimime river.

INTRODUCTION

In recent decades, the intensive use of chromium in various industrial activities has resulted in a contamination of aquatic ecosystems. Chromium contamination of water, soil or sediment is a major environmental concern due to its potential to enter the food chain (Hashem et al., 2020). Chromium occurs in different oxidation states from $-II$ to $+VI$. The trivalent (Cr(III)) and the hexavalent (Cr(VI)) forms are the major chromium species in aquatic systems. Cr(VI) is considered to be toxic due to its height oxidizing potential, elevated solubility and ability to cross biological membranes (Baraud et al., 2017). In soils, Cr(VI) species can be taken up by plants and easily leached out into the deeper soil layers causing groundwater and surface water pollution (James and Bartlett, 1984). They are also released from Cr(III) oxidation indirectly catalyzed by manganese oxides (Eary and Ral, 1987) or directly catalyzed by oxidants such as hydrogen peroxide or free oxygen (Kazakis et al., 2017). Cr(VI) species can be adsorbed by

iron oxyhydroxides, aluminium oxides and other soil colloids with a positively charged surface (James and Bartlett, 1983). Sediments play an important role in the aquatic ecosystems. They are considered to be the main sink for various pollutants, but when environmental conditions change (pH, redox potential, etc.), they can act as a source of pollution. Studies have been carried out on the fixation of Cr(VI) in serpentine sediments (Mpouras et al., 2017) and in sediments with illite and smectite predominance (Cao et al., 2021). The aim of this work is to study Cr(VI) fixation on sediments with a predominance of iron oxyhydroxysulphate, such as schwertmannite and jarosite and with a predominance of calcite.

MATERIAL AND METHODS

Sediments samples

In the present study, the chromium (VI) retention in the sediments of three rivers in

north-eastern Algeria was investigated. Two sediment samples were taken from a river in a mining area (Essouk river), and the third sample was taken from an urban area (Hemimime river) (Figure 1). The Essouk river located at Oum El Toub in the wilaya of Skikda, flows through the Sidi Kamber mining area. The main mineralogical components of the mine are galena (PbS), blende (ZnS) and barite (Boukhalfa, 1993). The Hemimime river located in the wilaya of Constantine, drains the industrial zone of the city of El-Khroub. Previous studies, have shown that the water of the Essouk river is characterized by an acidic pH (4.85), significant mineralization (2055 $\mu\text{s}/\text{cm}$), and high metals concentrations (Fe: 473 mg/l, Zn: 78.61 mg/l) (Boukhalfa, 2007), while the water of the Hemimime river is characterized by an alkaline pH (7.57). In the Essouk river, the sediment samples were taken in the immediate vicinity of the mine's effluents. The first sediment sample has a yellowish color (S1), the second one is red (S2). The sediment collected in the Hemimime river (S3) is brown in color. The sediments in the sampling areas are acidic in the case of the

Essouk samples (S1: 3.14; S2: 2.47) (Boukemara et al., 2017) and alkaline pH (7.84) with high content of organic matter (6.2%) in the case of Hemimime sample (Merabet et al., 2016). EDX analysis has shown the predominance of silicon, sulphur, potassium and iron in the case of the first Essouk sediment (S1), iron, silicon, and sulphur in the case of the second Essouk sediment (S2) (Boukhalfa and Chaguer, 2012) and carbon, silicon and calcium in the case of Hemimime sediment (S3). XRD analysis has shown that the main mineralogical phases of the sampled sediments are jarosite ($\text{KFe}_3(\text{SO}_4)_2(\text{OH})_6$) and quartz (SiO_2) in the case of the first Essouk sediment (S1), schwertmannite ($\text{Fe}_8\text{O}_8(\text{OH})_6 \cdot n\text{H}_2\text{O}$) and kaolinite ($\text{Al}_2\text{Si}_2\text{O}_5(\text{OH})_4$) in the case of the second Essouk sediment (S2) (Boukemara et al., 2017) and calcite (CaCO_3), quartz and kaolinite in the case of the Hemimime sediment (S3) (Merabet et al., 2016). The pH_{PZC} values are 4.38 and 4.66 for the sampled sediments S1 and S2 respectively (Boukemara et al., 2017) and 8.5 in the case of the sediment S3 (Talhi et al., 2020). The surface charge is therefore favorable for electrostatic

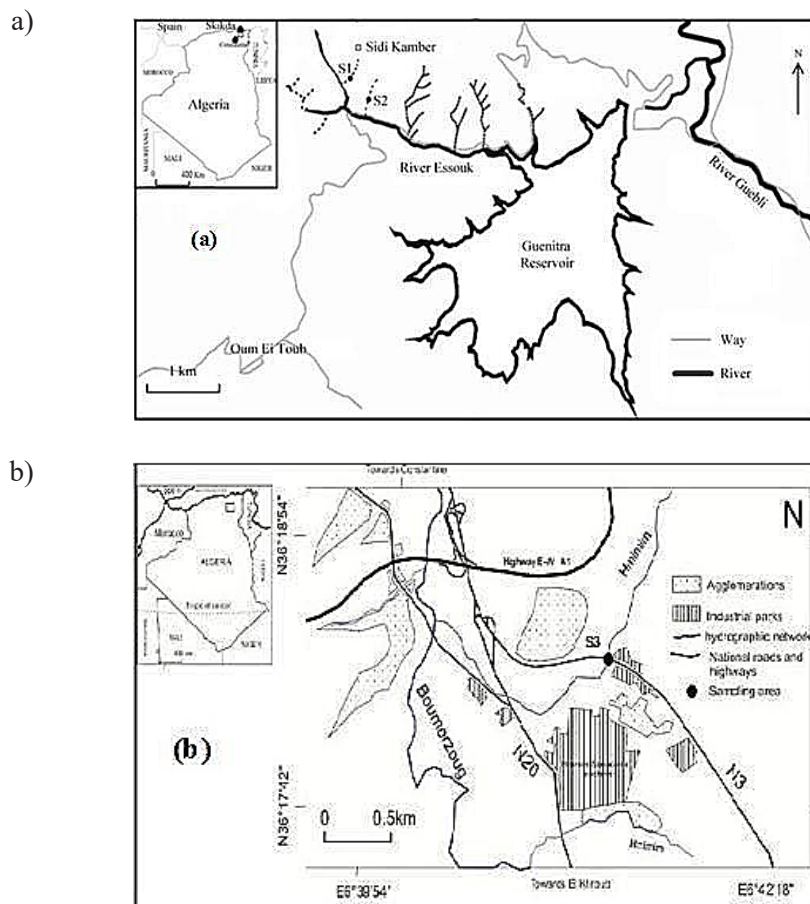


Figure 1. Localization of sediment sampling sites: (a) in the Essouk river; (b) in the Hemimime rivers

attraction of anions at $\text{pH} < 4.38$ for the sediment S1, at $\text{pH} < 4.66$ for the sediment S2, and at $\text{pH} < 8.5$ for the sediment S3.

Chromium (VI) fixation on sediments

Cr(VI) adsorption experiments were carried out in batch mode. Cr(VI) solutions were prepared from hydrated sodium dichromate ($\text{Na}_2\text{Cr}_2\text{O}_7 \cdot 2\text{H}_2\text{O}$). The effect of pH was evaluated in the pH range 2–10 with an initial Cr(VI) concentration of $1 \text{ mg} \cdot \text{L}^{-1}$ and a sediment dose of $1 \text{ g} \cdot \text{L}^{-1}$. The pH of the suspensions formed with Cr(VI) solution and sediments was adjusted using HCl (0.1M) and NaOH (0.1M). In the kinetic study, the suspensions formed Cr(VI) ($1 \text{ mg} \cdot \text{L}^{-1}$) solution and sediments (0.05 g), were stirred for times varying from 5 minutes to 24 hours. The effect of initial Cr(VI) concentration was studied for sediments dose of $1 \text{ g} \cdot \text{L}^{-1}$ and chromium concentrations $\leq 5 \text{ mg} \cdot \text{L}^{-1}$ during 24 hours of time. In all cases, the residual Cr(VI) concentration was determined in the supernatants obtained by centrifugation using the diphenylcarbazide method. In this method, hexavalent chromium reacts with diphenylcarbazide in slightly acidic solution to give a red-violet color which can be determined by molecular absorption spectrometry at 540 nm. The measurements were carried out using a SCHIMADZU 1650 PC double beam spectrophotometer.

RESULTS AND DISCUSSION

Effect of pH

The evolution of chromium (VI) fixation over the solution pH depends on the sediment

composition (Figure 2). The adsorption percentage does not exceed 12% for the predominantly jarosite sediment (S1) and 21% for the predominantly calcite sediment (S3). The presence of quartz in the first Essouk sediment (S1) and both quartz and kaolinite in the Hemimime sediment (S3) reduces their adsorption capacity. The negative charge on the surfaces of these minerals is responsible for their low anion adsorption capacity. Low Cr(VI) adsorption capacity has also been found in the case of soils characterized by a significant presence of quartz (Zhou and Chen, 2000). The significant presence of organic matter in the Hemimime sediment (S3) may also contribute to the reduction of Cr(VI) adsorption. It has been shown that soil organic matter facilitates the inhibition of Cr(VI) adsorption (Hua et al., 2020). In the case of the predominantly schwertmannite sediment (S2), a percentage of about 97% is reached showing an important efficiency for Cr(VI) retention. The pH has no effect at $\text{pH} < 8$ in the case of calcite predominance (S3). According to the pH_{PZC} of the sampled sediments, the interaction of Cr(VI) with the predominantly calcite sediment seems to be mainly electrostatic as the pH_{PZC} of this sediment is 8.5. However, in the case of the two others sediments, electrostatic interaction is not the sole mechanism which can explain Cr(VI) uptake; the intervention of chemical interaction is more likely, since their pH_{PZC} are 4.38 and 4.66 respectively and significant Cr(VI) adsorption is observed at pH values higher than these. Cr(VI) adsorption by sediments dominated by schwertmannite or jarosite, is maximal in the pH range 6–7. In a study concerning Cr(VI) adsorption on schwertmannite alone, the optimum pH was found to be 5 (Li et al., 2021). At $\text{pH} < 3.5$,

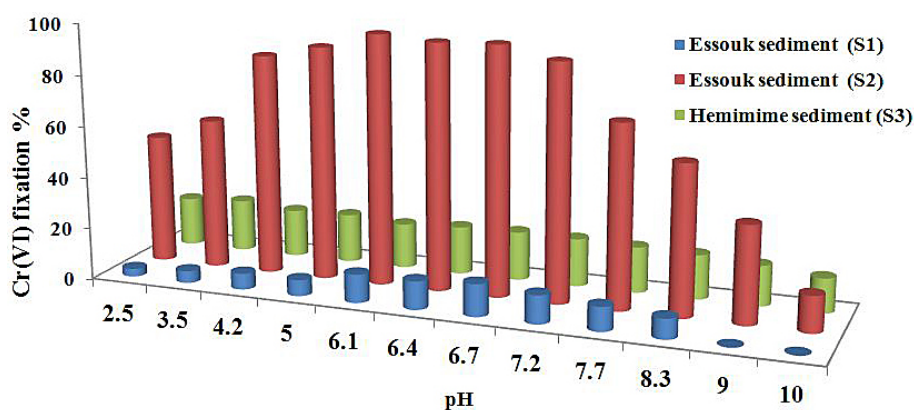


Figure 2. Effect of pH on Cr(VI) fixation in sediments ($C_0 = 1 \text{ mg/L}$; sediment dose – 1 g/L)

although anions adsorption is favored by the positive charge of the sediment surfaces, lower Cr(VI) adsorption is observed in both cases. The Cr(VI) speciation in this pH range is responsible for this anomaly. The presence of $\text{Cr}_2\text{O}_7^{2-}$, which is larger than HCrO_4^- , implies lower adsorption. In the pH range 7–8, the predominance of CrO_4^{2-} which requires more energy and occupies more active sites (Yu et al., 2020; Xu et al., 2019), explains the decrease in the fixation rate of Cr(VI) on the used sediments. In the three cases, the adsorption capacity gradually decreases at $\text{pH} > 8$ due to the competition of hydroxyl ions for adsorption. A similar observation has also been reported for the adsorption of Cr(VI) on serpentine sediments (Mpouras et al., 2017).

Kinetic study

The kinetics of Cr(VI) uptake by the studied sediments is characterized by two steps (Figure 3). The first fast step is related to the high Cr(VI) concentration gradient and to the availability of the adsorption sites. As the contact time increases, the Cr(VI) adsorption slows down due to the decrease of the available adsorption sites on the one hand and to the slow-down of Cr(VI) transport to the sediment surfaces on the other hand. The same kinetic evolution has been observed in the case of Cr(VI) adsorption on different soils (Zhou and Chen, 2000) and sediments (Cao et al., 2021). Cr(VI) adsorption on the second Essouk sediment where schwertmannite predominates

(S2), is faster, reaching equilibrium after 3 hours. However, in the case of jarosite (S1) or calcite (S3) predominance, it is reached after 5 hours.

In order to obtain information about the adsorption mechanism, several kinetic models were applied to analyze the experimental data. Assuming that Q_t ($\text{mg}\cdot\text{g}^{-1}$) and Q_e ($\text{mg}\cdot\text{g}^{-1}$) are the adsorbed amounts at time t and at equilibrium, the linear equations of the models are respectively:

- Pseudo-second order equation:

$$\frac{t}{Q_t} = \frac{1}{K Q_e^2} + \frac{1}{Q_e} (t) \quad (1)$$

where: K – the pseudo-second order rate constant ($\text{g}\cdot\text{mg}^{-1}\cdot\text{min}^{-1}$).

- Film diffusion equation:

$$\ln\left(1 - \left(\frac{Q_t}{Q_e}\right)\right) = -kt \quad (2)$$

where: k – diffusion constant (min^{-1}).

- Intraparticle diffusion equation:

$$Q_t = k\sqrt{t} + C \quad (3)$$

where: k – intraparticle diffusion constant ($\text{mg}\cdot\text{g}^{-1}\cdot\text{min}^{-1/2}$), C – a constant.

According to the calculated correlation coefficients (Table 1), the pseudo-second order model seems to be the best model to describe

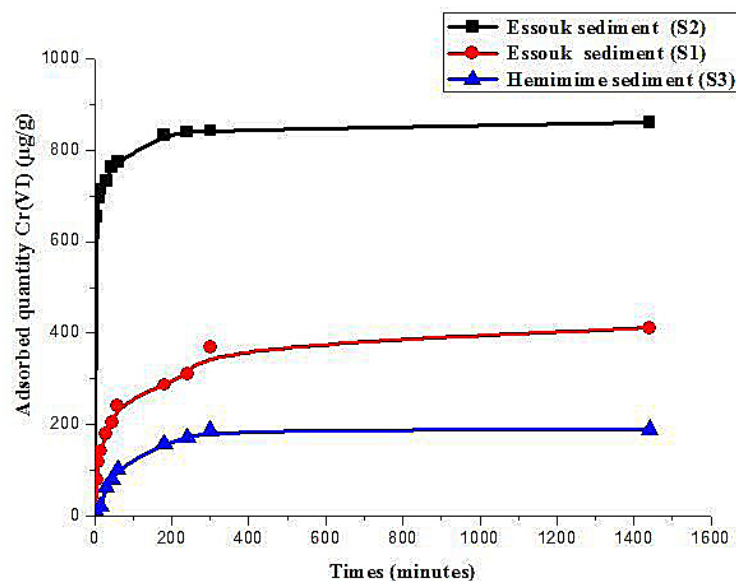


Figure 3. Effect of contact time on Cr(VI) fixation in sediments ($C_0 = 1 \text{ mg/L}$; sediment dose – 1 g/L)

the Cr(VI) adsorption kinetics in all cases. In this model the adsorption rate is directly proportional to the number of active sites of the adsorbent. It suggests the existence of chemisorption and assumes heterogeneity of binding sites with constant adsorption energy, the independence of site coverage rate and no interaction between adsorbed molecules. The same model has also well described the adsorption of Cr(VI) on the kaolinite (Dim et al., 2021) which is one of the constituents of the first Essouk sediment (S1) and the Hemimime sediment, on the schwertmannite (Li et al., 2021) which is dominant in the case of the second Essouk sediment (S2), and on calcite (Granados-Correa et al., 2013) which is the dominant phase in the case of Hemimime sediment (S3). The highest rate constant calculated by the pseudo-second-order equation is obtained in the case of the sediment dominated by schwertmannite ($K: 0.265 \text{ mg} \cdot \text{g}^{-1} \cdot \text{min}^{-1}$). This value is about four times higher than that calculated for the jarosite dominated sediment and two times higher than that calculated for the calcite dominated sediment. The diffusion models can also describe the kinetics of Cr(VI) adsorption on the studied sediments. The correlation coefficients calculated for these models are greater than 0.9 (Table 1). In the cases of jarosite predominance (S1) and calcite predominance (S3), Cr(VI) ions reach the sediment surfaces faster than they can diffuse into the adsorption sites. The corresponding kinetics is best described by the intraparticle diffusion model. Conversely, in the case of shewertmanite predominance (S2), Cr(VI) diffusion from the solution appears to be slower than diffusion to the adsorption sites. The kinetics is best described by the film diffusion model. In this model, the adsorbate passes through a layer of liquid film during adsorption and moves from this liquid phase to the final adsorption sites on the adsorbent surface.

Equilibrium study

The experimental isotherms of Cr(VI) adsorption on the first Essouk sediment with jarosite predominance (S1) and on Hemimime sediment with calcite predominance (S3) are of type S in the concentrations range tested (1 to 5 mg/l), showing that the adsorption is not limited by the number of active sites. In the case of the second Essouk sediment (S2) with schwertmannite predominance, the isotherm is of type L (Figure 4), which occurs when the attractive forces between the adsorbed molecules are weak.

The Langmuir, Freundlich and Henry isotherm models were tested to analyze the experimental equilibrium sorption data. Assuming that Q_e is the amount adsorbed at equilibrium (mg/g) and C_e is the concentration at equilibrium (mg/L), the linear equations of the tested models are as follows:

- Langmuir equation:

$$\frac{1}{Q_e} = \left[\left(\frac{1}{Q_{max} \cdot K} \right) \times \frac{1}{C_e} \right] + \frac{1}{Q_{max}} \quad (4)$$

where: Q_{max} – maximal adsorption capacity (mg/g), K – Langmuir constant (L/mg).

- Freundlich equation:

$$\text{Ln}Q_e = \text{Ln}K + (1/n) \text{Ln}C_e \quad (5)$$

where: K and n – are Freundlich constant and coefficient respectively.

- Henry equation:

$$Q_e = K_d C_e \quad (6)$$

where: K_d – distribution coefficient.

According to the calculated correlation coefficients, the Henry model which describes a linear dependence between adsorption capacity

Table 1. Kinetic parameters of Cr(VI) adsorption on sediments

Model	Pseudo second order	Intraparticle diffusion	Film diffusion
S1	R ² : 0.996 K: 0.058	R ² : 0.941 K: 0.016	R ² : 0.916 K: 0.006
S2	R ² : 0.999 K: 0.265	R ² : 0.912 K: 0.012	R ² : 0.959 K: 0.008
S3	R ² : 0.994 K: 0.135	R ² : 0.956 K: 0.011	R ² : 0.929 K: 0.012

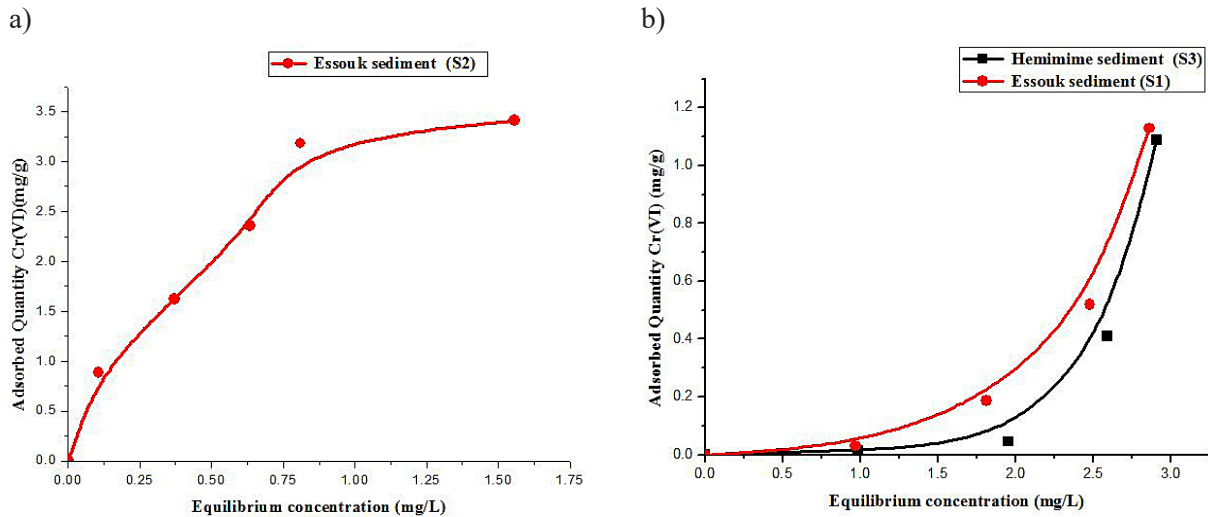


Figure 4. Adsorption isotherms of Cr(VI) in sediments (sediment dose – 1 g/L; time – 24 hours)

Table 2. Correlation coefficients of the isotherm models

Model	S1	S2	S3
Langmuir	0.965	0.957	0.986
Freundlich	0.985	0.947	0.783
Henry	0.733	0.758	0.510

and equilibrium concentration (Cao et al., 2021), cannot describe Cr(VI) adsorption on the studied sediments. The corresponding calculated correlation coefficients are low (Table 2). In the case of the Essouk sediments (S1 and S2), the Cr(VI) adsorption isotherms can be well described by both the Langmuir and Freundlich equations. The corresponding calculated correlation coefficients are higher than 0.9. The first model suggests a monolayer adsorption with identical adsorption sites that are energetically uniform. However, the second model describes sorption on a heterogeneous surface and suggests that the binding sites are not equivalent. Cr(VI) adsorption on Hemimime sediment can only be described by the Freundlich model. This model has also well described the Cr(VI) adsorption on serpentine sediments (Mpouras et al., 2017) and on soils (Castro-Rodriguez et al., 2015).

CONCLUSION

The results obtained in the present study show that Cr(VI) adsorption on sediments is mainly related to their composition. The predominance of the jarosite and the presence of quartz, clays and organic matter imply a low fixation capacity. The presence of calcite relatively increases the

adsorption capacity of the sediments. The predominance of schwertmannite is responsible for a significant retention of Cr(VI) in the sediments. In this case, the diffusion of Cr(VI) to the adsorption sites is faster. In rivers where jarosite or calcite predominate in the sediments, the mobility of Cr(VI) is significant. Consequently, where these two minerals predominate, more attention should be paid to the containing Cr(VI) effluents, which require extensive treatment.

REFERENCES

1. Baraud F., Leleyter L., Lemoine M., Hamdoun H. 2017. Cr in dredged marine sediments: Anthropogenic enrichment, bioavailability and potential adverse effects. *Marine Pollution Bulletin*, 120(1–2), 303–308.
2. Boukemara L., Boukhalifa C., Azzouz S., Reinert L., Duclaux L., Amrane A., Szymczyk A. 2017. Characterization of phosphorus interaction with sediments affected by acid mine drainage-relation with the sediment composition. *International Journal of Sediment Research*, 32(4), 481–486.
3. Boukhalifa C. 1993. Contribution to the evaluation of the rate of contamination of the Guénitra dam (Skikda) by the metals of Fe, Mn, Zn, Pb, and Cd. Thesis of magister, Mentouri Constantine University, Algeria.

4. Boukhalfa C. 2007. Heavy metals in the water and sediments of Oued Es-Souk, Algeria, a river receiving acid effluents from an abandoned mine. *African Journal of Aquatic Science*, 32(3), 245–249.
5. Boukhalfa C., Chaguer M. 2012. Characterisation of sediments polluted by acid mine drainage in the northeast of Algeria. *International Journal of Sediment Research*, 27, 402–407.
6. Cao Y., Dong S., Dai Z., Zhu L., Xiao T., Zhang X., Yin S., Soltanian M.R. 2021. Adsorption model identification for chromium (VI) transport in unconsolidated sediments. *Journal of Hydrology*, 598, #126228.
7. Castro-Rodriguez A., Carro-Perez M.E., Iturbe-Arguelles R., Gonzalez-Chavez J.L. 2015. Adsorption of hexavalent chromium in an industrial site contaminated with chromium in Mexico. *Environmental Earth Sciences*, 73, 175–183.
8. Dim P.E., Mustapha L.S., Termtanun M., Okafor J.O. 2021. Adsorption of chromium (VI) and iron (III) ions onto acid-modified kaolinite: Isotherm, kinetics and thermodynamics studies. *Arabian Journal of Chemistry*, 14(4), #103064.
9. Eary L.E., Rai D. 1987. Kinetics of chromium(III) oxidation to chromium(VI) by reaction with manganese dioxide. *Environmental Science and Technology*, 21, 1187–1193.
10. Granados-correa F., Garcia-alcantara E., Jimenez-becerril J. 2013. Study of Co (II) and Cr (VI) Adsorption from Aqueous Solution by CaCO₃. *Journal of The Chemical Society of Pakistan*, 35(4), 1088–1095.
11. Hashem M.A., Hasan M., Momen M.A., Payel S., Nur-A-Tomal M.S. 2020. Water hyacinth biochar for trivalent chromium adsorption from tannery wastewater. *Environmental and Sustainability Indicators*, 5, #100022.
12. Hua H., Zhao Z., Xu R., Chang E., Fang D., Dong Y., Hong Z., Shi R., Jiang J. 2020. Effect of ferrolysis and organic matter accumulation on chromate adsorption characteristics of an Oxisol-derived paddy soil. *Science of the Total Environment*, 744, #140868.
13. James B.R., Bartlett R.J. 1983. Behavior of chromium in soils: VII. Adsorption and reduction of hexavalent forms. *Journal of Environmental Quality*, 12, 177–181.
14. James B.R., Bartlett R.J. 1984. Plant-soil interactions of chromium. *Journal of Environmental Quality*, 13, 67–70.
15. Kazakis N., Kantiranis N., Kalaitzidou K., Kaprara E., Mitrakas M., Frei R., Vargemezis G., Tsourlos P., Zouboulis A., Filippidis A. 2017. Origin of hexavalent chromium in groundwater: The example of Sarigkiol Basin, Northern Greece. *Science of the Total Environment*, 593–594, 552–566.
16. Li X., Guo C., Jin X., He C., Yao Q., Lu G., Dang Z. 2021. Mechanisms of Cr(VI) adsorption on schwertmannite under environmental disturbance: Changes in surface complex structures. *Journal of Hazardous Materials*, 416, 125781.
17. Merabet S., Boukhalfa C., Chellat S., Boultif A. 2016. Characterization of Chromium (III) Removal from Water by River bed Sediments – Kinetic and Equilibrium studies. *Journal of Materials and Environmental Science*, 7(5), 1624–1632.
18. Mpouras T., Chrysochoou M., Dermatas D. 2017. Investigation of hexavalent chromium sorption in serpentine sediments. *Journal of Contaminant Hydrology*, 197, 29–38.
19. Talhi A., Merabet S., Bouhouf L., Boukhalfa C. 2020. Removal of Acid black 210 by adsorption on calcite. *Desalination and Water Treatment*, 205, 407–411.
20. Xu Y., Chen J., Chen R., Yu P., Guo S., Wang X. 2019. Adsorption and reduction of chromium(VI) from aqueous solution using polypyrrole/calcium rectorite composite adsorbent. *Water Research*, 160, 148–157.
21. Yu Z., Song W., Li J., Li Q. 2020. Improved simultaneous adsorption of Cu(II) and Cr(VI) of organic modified metakaolin-based geopolymer. *Arabian Journal of Chemistry*, 13(3), 4811–4823.
22. Zhou D.M., Chen H.M. 2000. CrVI adsorption on four typical soil colloids: equilibrium and kinetics. *Journal of Environmental Sciences*, 12(3), 325–329.